JOURNAL OF Applied Polymer SCIENCE

# Incorporation of Multiwalled Carbon Nanotube into a Polymethacrylate-Based Monolith for Ion Chromatography

**Nani Wang,[1] Shiwei He,[2] Wenwu Yan,[1] Yan Zhu[1]**

[1]Department of Chemistry, Xixi Campus, Zhejiang University, Hangzhou 310028, People's Republic of China

[2]Institute of Scientific and Technical Information of Zhejiang Province, Hangzhou 310006, People's Republic of China

Correspondence to: Y. Zhu (E-mail: zhuyan@zju.edu.cn)

**ABSTRACT:** A new monolithic stationary phase containing multiwalled carbon nanotube (MWCNT) was prepared by *in situ* polymerization of methacrylate monomers in a silanized capillary. The novel stationary phases were studied by scanning electron microscopy, Raman spectroscopy, thermogravimetric analysis, Fourier Transform Infrared spectroscopy, and mechanical stability test. Application of the columns in ion chromatography (IC) separation of five inorganic anions provided satisfactory under the isocratic elution condition. It was observed that MWCNT in the monoliths played an important role in the IC separation. Both the column efficiencies and exchange capacities were improved by adding MWCNT in the monoliths. © 2012 Wiley Periodicals, Inc. J. Appl. Polym. Sci. 000: 000–000, 2012

**KEYWORDS:** carbon nanotube; monolith; composite; ion exchanger; chromatography

Received 17 August 2011; accepted 16 March 2012; published online
**DOI: 10.1002/app.37722**

## INTRODUCTION

Porous monolithic materials that have merged in early 1990s have become popular as stationary phases for reversed-phase chromatography,[1] hydrophobic interaction chromatography,[2] affinity chromatography,[3] and capillary electrochromatography (CEC).[4] Monolithic columns have high permeability,[5] which enables excellent performance in the fast separation of large molecules such as proteins,[6] DNA,[7] and synthetic polymers.[4] However, monolithic columns showed poor separation performance of small molecules and ions due to the lack of small pores in monolithic structures.[8] Therefore, monolithic columns have overwhelmingly been applied in the isolation of large bimolecules from complex samples, and until recently have received only limited attention in separation of small molecules and ions.[5,8,9] Hence, the design of novel monolith material for the separation of small ions species has been a demanding challenge in separation science.

Ion chromatography (IC) was popularly used for the analysis of different kinds of ions at present. Following the recent reports of polymer monoliths for IC, several methods have been published for the synthesis of novel stationary phases. Some groups[10,11] have attempted to obtain monolithic ion exchangers by dynamically modifying or permanently coating reversed-phase monoliths with liquid ion exchangers. However, the application of this approach was limited by the variations in coating stability and intolerance of the coated phase to changes in mobile phase composition and column temperature.[9] To overcome these drawbacks, some groups[12,13] prepared stationary phases with covalently bonded ion exchange groups, such as anion-exchange quaternary amino group, cation-exchange sulfuric acid group, and zwitterionic molecules.

Besides these approaches, an alternative way to increase the column efficiency may be achieved by incorporation of nanomaterials, especially carbon nanotubes (CNTs) in monolith materials. CNTs hold a great potential for achieving efficient separations performance owing to their unique properties, such as high surface area, porous nature, low density, high strength, extraordinary thermal properties, and special functional properties.[8,14] Due to their excellent properties, CNTs are expected to be a promising material in many areas, such as microelectrode,[15] catalyst,[16] sensor,[17] optical limiter,[18] composite material,[19] sorbent,[20] and so on.

In the field of chromatography, the use of CNTs as stationary phase has been pursued for gas chromatography,[21] liquid chromatography,[7,8] and CEC.[22] Our previous work[23] demonstrated advantages of incorporation of CNTs in packing columns for

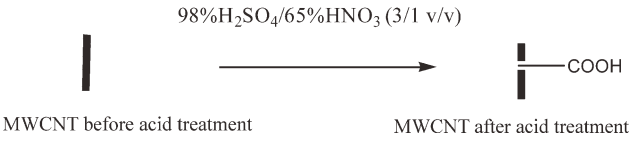


**Figure 1.** Purification of MWCNT.

reversed-phase chromatography, including excellent mechanical stability, high surface area, and good chromatography performance on separation of anions and small molecules. In the field of polymer monoliths, CNTs were entrapped in capillary columns to enhance separation performance for small molecules in the reversed phase.[8] The addition of CNTs increased both retention and column efficiency of the capillary columns. Nevertheless, the application of CNTs in IC monolithic columns has not been reported.

The aim of this work was to investigate a novel IC stationary phase by combining CNTs and monolith materials. Multiwall carbon nanotubes (MWCNT) were entrapped in the poly(glycidyl methacrylate-*co*-ethylene dimethacrylate) monoliths. Then, the porous polymer monoliths were modified by trimethylamine. Furthermore, the effects of MWCNT in the complete anion-exchange columns were studied in detail.

## EXPERIMENTAL

### Apparatus and Instrumentations

All chromatographic tests were carried out using a homemade IC system including a pump (WellChrom HPLC-Pump K-120, Knauer, Germany), a microsample injector with 0.5 $\mu$L sample rotor (Model 7520 Syringe-Loading Injector, Rheodyne, Cotati, CA), and a variable-wavelength UV detector (655A, Hitachi, Japan). Data were collected with Sepu 3000 chromatogram work station (Puhui Sci. Tech. Co., China). Each injection was repeated at least twice.

The scanning electron microscopy (SEM) images were obtained using a HITACHI S-4700 field emission scanning electron microscope (Hitachi, Japan). The Raman spectra were taken on Labor Raman HR-800 Raman Spectrometer (Jobin Yvon, France). The thermogravimetric analysis (TGA) was carried out on SDT Q600 TA instrument (TA) under a nitrogen atmosphere from 40°C to 500°C. FTIR spectra were recorded in the range 400–4000 $cm^{-1}$ on a Bruker VECTOR-22 FTIR spectrophotometer (Bruker, Germany) using KBr pellets.

### Chemicals and Solvents

All the chemicals used in this study were analytical standard grade. Glycidyl methacrylate (GMA, >98%) and ethylene dimethacrylate (EDMA, >98%) were pursued from Shanghai Reagent Company (Shanghai, China). MWCNT (sample purities: >95%) with the average outer diameter (OD) about 10 nm were obtained from the Institute of Material Physics and Microstructure of Zhejiang University, China. Azobisisobutyronitrile (AIBN, Shanghai Chemical Reagent Co., China, >99%) was recrystallized from anhydrous alcohol. 1-Propanol (>99%), trimethylamine (30% in $H_2O$, v/v) and 1, 4-butanediol (>99%) were bought from Kelong Chemical Reagent Co. (Chengdu, China). Anhydrous alcohol (>99%) and acetic acid (>99%) were obtained from Guangfu Chemical Reagent Co. (Tianjin, China).$\gamma$-Methacryloxypropyl trimethoxysilane ($\gamma$-MAPS,>98%) was from Nanjing Chemical Reagent Co. (Nanjing, China). Deionized water used was purified by Millipore Simplicity (Millipore, France) to 18.2 MΩ. The 520-$\mu$m id fused-silica capillary was purchased from Yongnian Optic Fiber Plant (Hebei, China).

### Purification of MWCNT

MWCNT was purified as follows[8]: MWCNT (100 mg) was suspended in the mixture of concentrated $H_2SO_4$/$HNO_3$ (3 : 1, v/v, 100 mL) in a 250 mL flask and refluxed in a water bath for 2 h at 60°C, as illustrated in Figure 1. The resulting suspension was then diluted with water and washed until the pH value reached 7. After filtration, the resulting acid-treated MWCNT was dried in vacuum at 30°C for 24 h.

### Silanization of the Capillary's Inner Wall

The pretreatment of the fused-silica capillaries were carried out as follows.[24] First, siloxane groups at the inner surface of raw fused-silica capillaries were hydrolyzed first to increase the density of silanol groups serving as anchors for subsequent silanization. A new, bare capillary columns was rinsed with NaOH aqueous solution (1.0 mol/L) and successively washed with pure water, HCl (0.1 mol/L), pure water, acetone, and subsequently dried with nitrogen gas for 12 h at a pressure of 10 psi.

Second, the inner wall of the fused-silica capillary was then treated with $\gamma$-MAPS to provide anchoring sites for the grafting of polymer to the capillary surface and enhancing wetting of the surface by the monomer mixture. The clean, bare capillary was then filled with a solution of $\gamma$-MAPS (1.0 mL), ethanol (1.0 mL), and acetic acid (0.2 mL) and was kept at 40°C for 24 h to complete silanization, as illustrated in Figure 2.

Finally, the capillary was rinsed with acetone, and dried by nitrogen gas for 24 h at a pressure of 10 psi.

### Preparation of Porous Polymer Monoliths in Fused-Silica Capillaries

There were three monolithic columns in this study. The first column ($C_{0\%MWCNT}$) was prepared as follows: a polymerization mixture containing GMA (0.9 mL), EDMA (0.3 mL), 1-

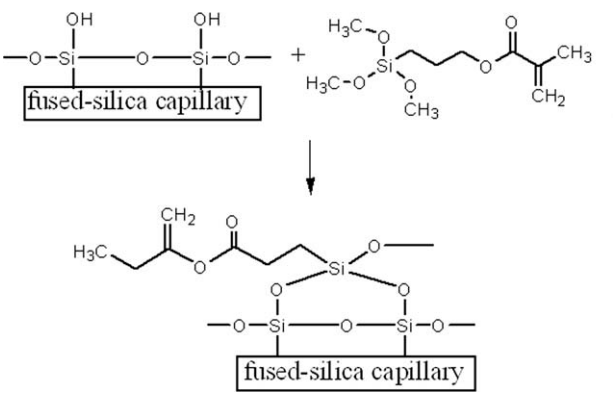


**Figure 2.** Silanization of the capillary's inner wall.

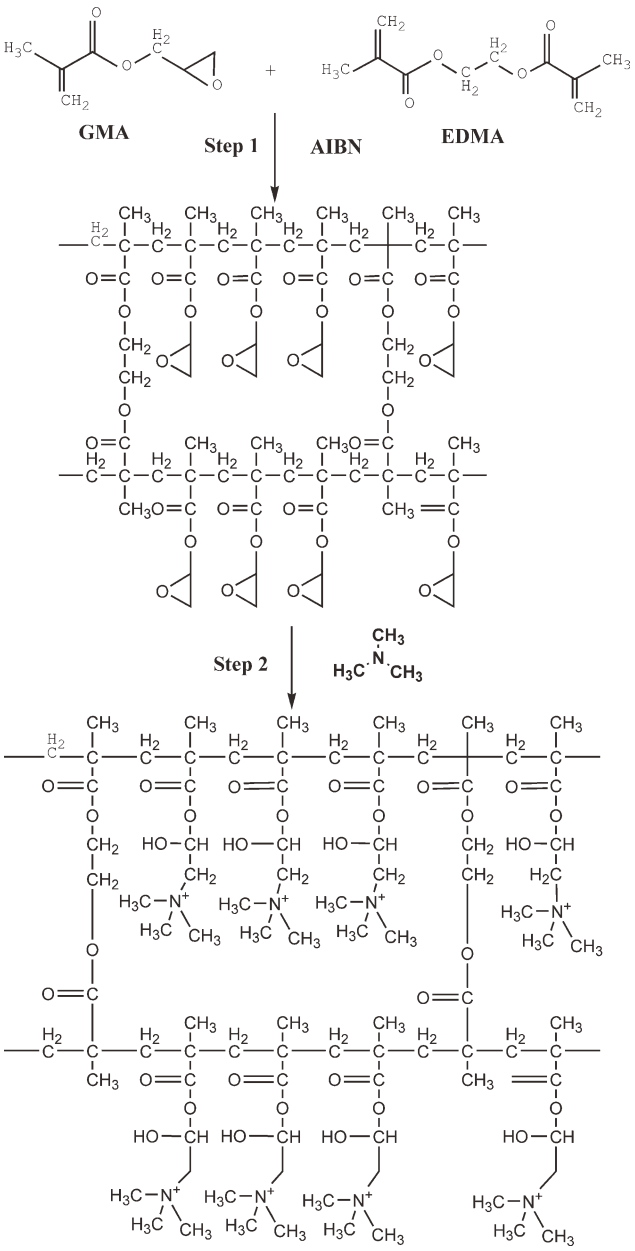


**Figure 3.** Reaction scheme for the preparation of anion-exchange monolithic columns.

propanol (1.05 mL), 1,4-butanediol (0.6 mL), water (0.15 mL), and AIBN (0.0120 g) was purged with nitrogen for 10 min, and then a 20-cm piece of the silanized capillary was filled with the mixture. After sealing both ends of the capillary, the column was left to polymerize at 55°C for 24 h, as illustrated in Figure 3. After polymerization, the column was washed with ethanol for at least 24 h.

The second column ($C_{0.2\%MWCNT}$) was synthesized as follows: acid-treated MWCNT (0.0229 g) was completely suspended in 1-propanol (10 mL) under ultrasonic treatment. Then, the suspension (1.05 mL) was added into the polymerization mixture containing GMA (0.9 mL), EDMA (0.3 mL), 1-propanol, 1,4-butanediol (0.6 mL), water (0.15 mL), and AIBN (0.0120 g). The following preparation procedures of $C_{0.2\%MWCNT}$ was the same as that of $C_{0\%MWCNT}$. As a result, the content of MWCNT in $C_{0.2\%MWCNT}$ was 0.2 wt % (respect to monomers). The other composites of $C_{0.2\%MWCNT}$ were the same as that of $C_{0\%MWCNT}$. For the third column ($C_{0.5\%MWCNT}$), the content of MWCNT in $C_{0.5\%MWCNT}$ was 0.5 wt % (respect to monomers). The other composites and the preparation procedures of $C_{0.5\%MWCNT}$ were the same as those of $C_{0.2\%MWCNT}$.

### Modification of Porous Polymer Monoliths

In this study, the polymethacrylate-based monoliths were modified by the ring-opening of the epoxy groups through reaction with trimethylamine at 80°C, as illustrated in Figure 3. The 30% (v/v) aqueous solution of trimethylamine was pumped through the monolith at a flow rate of 2 $\mu$L/min for 2 h at 80°C. The monolith was then rinsed with water, followed by 80 mmol/L $NaClO_4$ solution by pumping each of them for at least 24 h at a flow rate 5 $\mu$L/min.

### Measurement of Exchange Capacity

The exchange capacity of the monolithic column was determined using nitrous anion adsorption/desorption.[25] The columns were loaded with $NaNO_2$ aqueous solutions (50 mmol/L) until saturation. The columns were then flushed with water to remove interstitial $NO_2^-$ and the bound $NO_2^-$ was eluted using sodium perchlorate aqueous solution (100 mmol/L), and determined by direct UV absorbance ($\lambda$ = 215 nm).

## RESULTS AND DISCUSSION

### Preparation of the Monoliths

The anion-exchange monolithic columns were synthesized via free radical polymerization of GMA and EDMA monomers and a subsequent ring-opening reaction of epoxy groups in GMA moiety. As both GMA and EDMA had unsaturated double bonds, free radical polymerization between them was easily conducted.[32] As shown in Figure 3, Step 1 was the

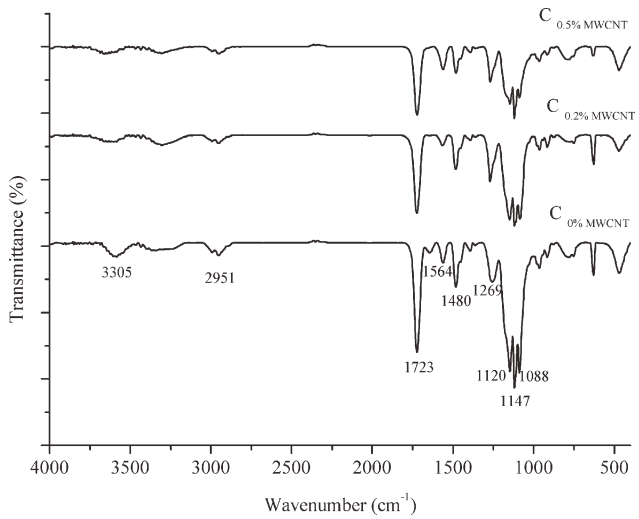


**Figure 4.** FTIR spectra of the polymer monolithic materials.

Applied Polymer SCIENCE

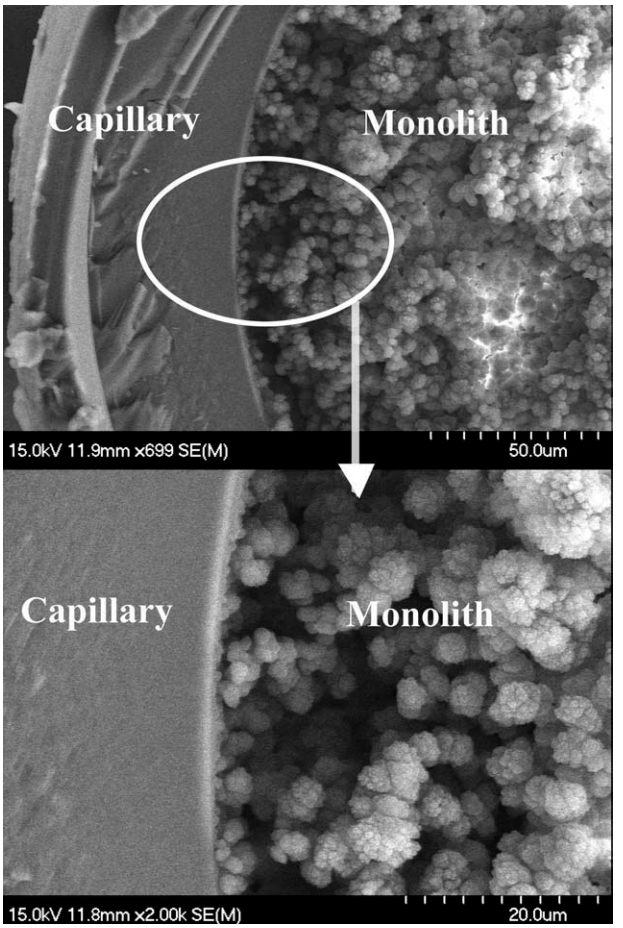


**Figure 5.** Effect of silanization of the fused-silica capillary on the attachment of the monolith ($C_{0.2\%MWCNT}$) to the capillary's inner wall (Top image: magnification ×699; bottom image: magnification ×2000).

copolymerization between GMA and EDMA, and Step 2 was the ring-opening reaction of epoxy groups in the porous polymer monolith. In Step 2, the epoxy groups were converted into positive charged —$N(CH_3)_3^+$groups in the polymer chains, which was confirmed by FTIR spectra (as shown in Figure 4).

All the spectra in Figure 4 showed a band at 1722 $cm^{-1}$ specific to carbonyl stretching vibration in ether and a weak band at 3100 and 3500 $cm^{-1}$, which was characteristic to the stretching vibration of —OH groups. The bands at 2985–3000 $cm^{-1}$ region characterized the valence vibration of —$CH_3$, —$CH_2$—, and —CH structures. The bands at 1564 and 1480 $cm^{-1}$ may be due to asymmetric and symmetric deformation of —$N^+(CH_3)_3$.[33] The band at 1269 $cm^{-1}$ corresponded to the stretching vibration of C—O bond, while the peaks at 1150–1080 $cm^{-1}$ were C—O—C stretching vibration.[34]

Application of porous monolith in chromatography relied on intimate contact with a surface that had the interacting sites. For example, quaternary ammonium groups on the surface of the monoliths enabled the separation of anions on the monolithic columns using anion-exchange mode. To obtain a large surface area, a large amount of pores should be incorporated into the monolith. Furthermore, the pores in the polymer allowed mobile phase to flow through the monolith at a reasonable pressure. In fact, a porogen agent was essential for the size and distribution of the pores. In this work, a ternary porogen system (a mixture of propyl alcohol, 1.4-butanediol, and water) was selected due to its good solubility in monomer mixture and excellent performance during the polymerization.[35]

Moreover, the modification of the fused-silica capillary was essential for the preparation of monoliths. The inner wall was treated with silane agents to provide anchoring sites for the grafting of polymer to the capillary surface and enhancing wetting of the surface by the monomer mixture. In this work, $\gamma$-MAPS was used to introduce C=C groups to the inner wall of the capillary. First, the bare capillary was activated by 1.0 mol/L NaOH to increase the amount of silanol groups available to react with $\gamma$-MAPS. Then the capillary was filled with a mixture of $\gamma$-MAPS and acetic acid aqueous solution and left in the water bath for 24 h. The acetic acid solution was used to provide a suitable pH for the silanization.[36] The SEM images presented in Figure 5 illustrated that silanization facilitates a strong attachment between the silica surface and the methacrylate monolith. The covalent interaction between the monolith and capillary imparted stability to the columns, as already discussed in the literature.[37]

### Raman Characterization

The Raman spectra were carried out to characterize the chemical composition before and after incorporation of MWCNT. Figure 6 showed the Raman spectra of the three monolithic materials and MWCNT in the spectral ranges from 800 to 1800 $cm^{-1}$. The broad band at 1300–1400 $cm^{-1}$ known as "D" band, associated with the disorder state in graphite compounds and another one called "G" band at 1500–1600 $cm^{-1}$ assigned to tangential vibration mode were located in the spectra of MWCNT.[23] The Raman intensity rose at the wave number of 1350 and 1580 $cm^{-1}$ in $C_{0.2\%MWCNT}$ and $C_{0.5\%MWCNT}$ rather than the $C_{0\%MWCNT}$, indicating that the incorporation of MWCNT caused the spectral changed.

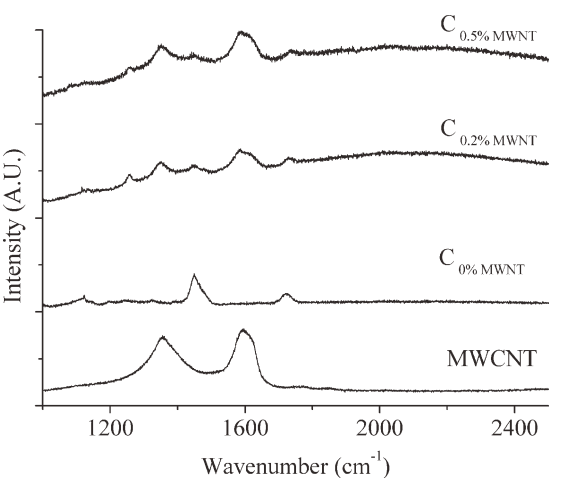


**Figure 6.** Raman spectra of the monoliths and MWCNT.

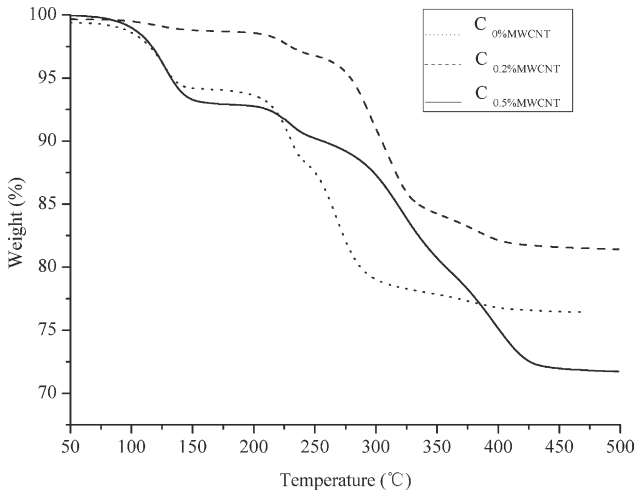


**Figure 7.** TGA curves of the monolithic materials.

### Thermal Analysis

According to the previous literatures, high temperature could accelerate the decomposition of anion-exchange polymers, especially the polymer containing quaternary ammonium groups. The thermal degradation was demonstrated as follows.[39] When the temperature was above approximately 200°C, the quaternary ammonium groups began to cleave from the backbone of the polymer. Then the —C=O and C—O—C groups in the copolymer thermally decomposed at higher temperature.

The thermal analysis conducted on the $C_{0\%MWCNT}$ (dot line), $C_{0.2\%MWCNT}$ (dash line), and $C_{0.5\%MWCNT}$ (solid line) were presented in Figure 7. As shown in Figure 7, the thermal degradation of the monolithic materials was a multistage process. The first stage, up to 150°C, the weight losses of three materials corresponded to the evaporation of the adsorbed water. According to the mechanism of thermal degradation,[33,39,40] the second stage (from 200 to 250°C) was attributed to the decomposition of quaternary ammonium groups. At this stage, all of the degradation temperature for $C_{0\%MWCNT}$, $C_{0.2\%MWCNT}$, and $C_{0.5\%MWCNT}$ were 230°C. Finally, thermal degradation in the range between 250°C and 350°C may be explained by the decomposition of C—O—C bridges and —C=O groups. At this stage, the decomposition temperature for $C_{0.2\%MWCNT}$ and $C_{0.5\%MWCNT}$ was observed to be slightly shift to a higher temperature (300–320°C) than that obtained with the $C_{0\%MWCNT}$ (~ 290°C) It may be attributed to the formation of covalent bonds between polymer and MWCNT[42] it was possible that the extraordinary thermal property of MWCNT may also contribute to this phenomenon.[23] However, the improvement was so inconspicuous resulting from the small amount of CNTs. If the content of nanotube could be increased, the thermal stability would be improved.

### Acid Treatment of MWCNT

Most production processes of MWCNT generated various carbonaceous particles, such as amorphous carbon, nanocrystalline graphites, and fullerenes, and final effluent includes transition metal catalysts.[38] The most common method to remove undesired by-products was acid treatment. Therefore, the mixture of concentrated nitric acid and concentrated sulfate acid was used in this work for the purification of MWCNT. In previous researches,[43–45] this acid treatment was reported to result in carbonyl, carboxyl, and hydroxyl groups on the CNT, but their locations were unknown. In this work, FTIR studies of raw and acid-treated MWCNT (as shown in Figure 8) indicated that this acid treatment also generated these functional groups on MWCNT: O—H groups (3447 $cm^{-1}$), C=O groups (1669 $cm^{-1}$)[43] and C—O groups (1118 $cm^{-1}$).[45] The band at 1542 $cm^{-1}$ was attributed to the phonon modes of CNTs.[44]

### Morphology of the Monoliths

Figure 9 showed the SEM images of the monoliths. The SEM micrographs showed significant differences in morphology among $C_{0\%MWCNT}$, $C_{0.2\%MWCNT}$, and $C_{0.5\%MWCNT}$. While the surface of the columns containing MWCNT ($C_{0.2\%MWCNT}$ and $C_{0.5\%MWCNT}$) was rather irregular, the surface of the bare column was relatively round and smooth. There were two possible reasons that could explain the differences. First, during the polymerization, poly(methy methacrylate) beads were decorated to the sidewall of MWCNT.[26,42] As a result, the size of particles in the monoliths containing MWCNT was much more irregular than that in $C_{0\%MWCNT}$. Second, the heterogeneous MWCNT with super-high curved surface could break the spherical surface of particles to result in nonspherical configuration.[42] Therefore, the shape of particles in $C_{0\%MWCNT}$ was relatively more regular and round. It was worth adding that MWCNT could not be found on the surface of $C_{0.2\%MWCNT}$ due to the low content of MWCNT in the monolith.

When the addition of MWCNT increased, some tubes were observed on the surface of $C_{0.5\%MWCNT}$. It may be explained by that although most of MWCNT existed inside the polymer, a few carbon tubes still protruded from the surface of the monolith and were coated with the copolymer.[26] As reported in the previous literatures,[26,41,42] various methacrylate copolymers have been used to coat CNT with different diameter. Since the OD of MWCNT used in this study was about 10 nm, the polymer coating had a thickness of approximately 800 nm. The FTIR spectra of MWCNT (Figure 8) indicated that there were

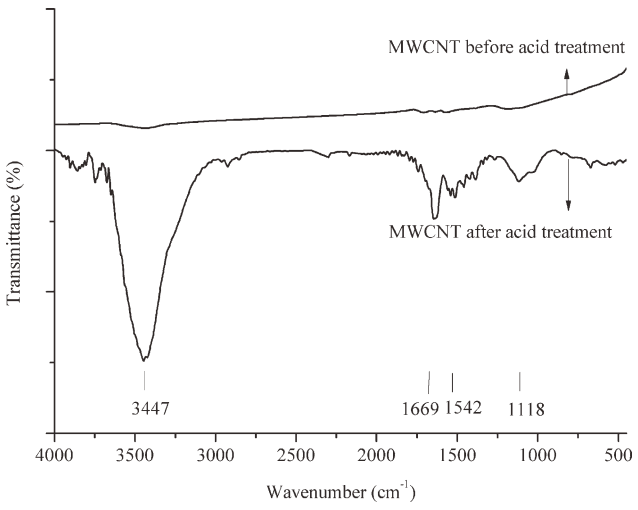


**Figure 8.** FTIR spectra of MWCNT before and after acid treatment.

Applied Polymer SCIENCE

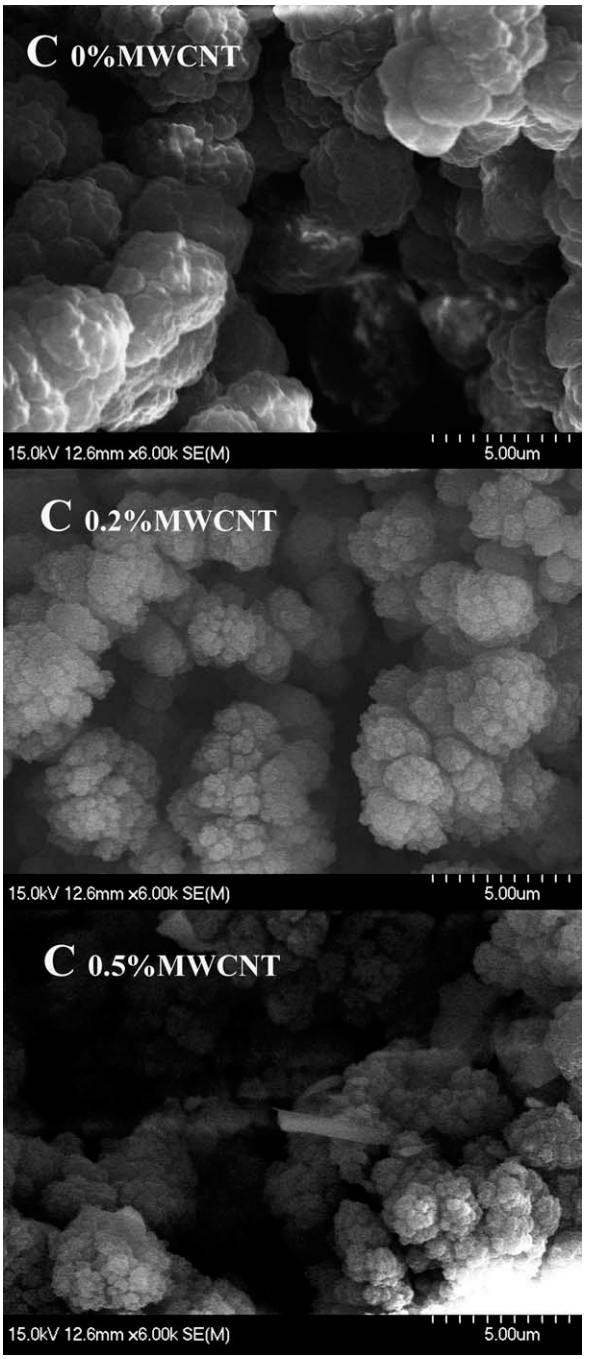


**Figure 9.** SEM images of the three monoliths.

carboxylic groups on the acid-treated MWCNT. The presence of GMA in the polymer provided the epoxy functional groups to which the acidic groups present on the surface of the MWCNT could covalently attach to form esters.[26] Therefore, the polymer coating on MWCNT may be explained by the reaction between carboxylic group and epoxy ring from the copolymer.

### Permeability and Exchange Capacity of the Monoliths

Figure 10 showed the back pressures of the columns at different flow rates. Water was used for the measurement of the pressure drop across the columns at different flow rates, which could be

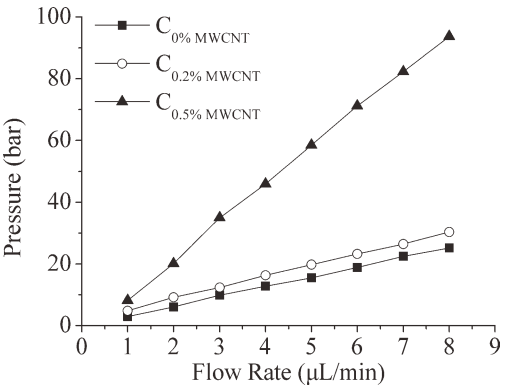


**Figure 10.** Plots of the volumetric flow rate of water against the back pressure of $C_{0\%MWCNT}$, $C_{0.2\%MWCNT}$, and $C_{0.5\%MWCNT}$.

used to indicate the mechanical stability and permeability of the columns.[27] For each measured column, the back pressures dependence on flow rate was a straight line with a correlation coefficient $R^2$ better than 0.999. It indicated that permeability and mechanical stability of the three monoliths were both excellent. From Figure 10, back pressures of the columns increased as the MWCNT content increased. $C_{0.5\%MWCNT}$ exhibited higher back pressures at all flow rates, compared to that of the other two columns. One possible reason for this was a reduction of pore size. To understand the differences in back pressure in the three columns, the total porosity ($\varepsilon_T$), permeability ($K^0$), and the mean pore diameter ($d_p$) were examined (Table I).

The porosity of the monoliths was examined by a flow method.[1,28] $\varepsilon_T$ was calculated using eq. (1).[28]

$$\varepsilon_T = \frac{V}{\pi r^2 c} \times 100\% \quad (1)$$

where $r$ was the inner radius of the empty capillary column, $V$ was the volumetric flow rate of the mobile phase, and c was the linear velocity of the mobile phase, which was determined by the water peak. The average value of the results obtained at different flow rates (2, 3, 4, 5, 6 $\mu$L/min) was regarded as the total porosity of the monolith.

$K^0$ was calculated using eq. (2).[1]

$$K^0 = \frac{c\eta L\varepsilon_T}{\Delta p} \quad (2)$$

where $c$ was the linear velocity of the mobile phase, $\eta$ was the dynamic viscosity of the mobile phase, $L$ was the effective column length, and $\Delta p$ was pressure drop.

**Table I.** Parameters for $C_{0\%MWCNT}$, $C_{0.2\%MWCNT}$, $C_{0.5\%MWCNT}$: Total Porosity ($\varepsilon_T$), Column Specific Permeability Index ($K^0$), and Pore Diameter ($d_p$)

| Monoliths | $\varepsilon_T$ (%) | $K^0$ ($10^{-15}$ m$^2$) | $d_p$ (μm) |
|---|---|---|---|
| $C_{0\%MWCNT}$ | 20.4 | 7.79 | 0.87 |
| $C_{0.2\%MWCNT}$ | 13.6 | 4.23 | 0.78 |
| $C_{0.5\%MWCNT}$ | 4.08 | 4.14 | 0.44 |

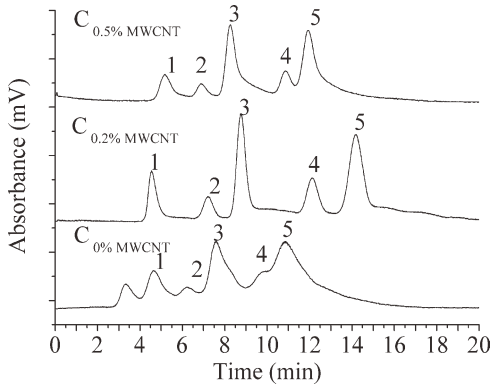


**Figure 11.** Comparison of separation of five anions on the $C_{0\%MWCNT}$, $C_{0.2\%MWCNT}$, and $C_{0.5\%MWCNT}$ at 6 $\mu$L/min using 80 mmol/L $NaClO_4$ as mobile phase. Peaks identification: (1) iodate; (2) bromate; (3) nitrite; (4) bromide; (5) nitrate. Absorbance was monitored at $\lambda = 215$ nm.

From the total porosity and specific permeability, the size of equivalent pore could be obtained by the Kozeny-Carman equation. $d_p$ was calculated using eq. (3).[28]

$$d_p = 2 \times \left( \frac{5 \times K^0}{\varepsilon_T} \right)^{1/2} \quad (3)$$

where $d_p$ was the mean pore diameter. The coefficient 5 was the empirical Kozeny coefficient for the pore structure and the factor 2 was the shape factor for cylindrical pores. Here, $K^0$ was tested with water as mobile phase for obtaining $d_p$.

Table I showed that increasing the MWCNT content dramatically decreased the total porosity of the columns and the pore size. One possible reason was that the polymer particles could be decorated to MWCNT during polymerization, resulting in relatively higher degree of cross-linking.[42] It was also likely that, the irregular and rugulose surface contributed to abundant small pores in the monolith.[8,9] This small pore size may exert a positive effect on the separation of small molecules.[8] However, this came at the cost of permeability, thus making the back pressure of $C_{0.2\%MWCNT}$ and $C_{0.5\%MWCNT}$ higher than that of $C_{0\%MWCNT}$.

### Chromatographic Performance

Glycidyl methacrylate was selected as monomer because its epoxy groups could be easily converted into various functional groups. After polymerization, the porous polymer monoliths were modified by trimethylamine, as shown in Figure 3. Therefore, there were quaternary ammonium groups on the surface of the monoliths. These strong anion-exchange groups (quaternary ammonium groups) enabled the separation of anions on the monolithic columns using anion-exchange mode.

The exchange capacity of the monolithic column was estimated using nitrous anion adsorption/desorption.[25] The exchange capacity for $C_{0\%\ MWCNT}$, $C_{0.2\%\ MWCNT}$, and $C_{0.5\%\ MWCNT}$ was 2.75, 4.00, 3.00 $\mu$equiv/m, respectively. $C_{0.2\%\ MWCNT}$ exhibited higher exchange capacity than $C_{0\%MWCNT}$. It was likely that, the irregular and rugulose surface contributed to the higher exchange capacity of the column. This finding correlated with some earlier observations,[25,29,30] where an irregular surface facilitated more efficient separation of proteins or nucleic acid. However, the exchange capacity of $C_{0.5\%\ MWCNT}$ was found to be lower than that of $C_{0.2\%\ MWCNT}$ despite more MWCNT in the monolith. It was speculated that this finding resulted from the poor permeability of $C_{0.5\%\ MWCNT}$. During the modification of the polymer monoliths, trimethlyamine solution flowed through the monolith rod. In this instance, the lack of large pores in $C_{0.5\%\ MWCNT}$ resulted in slow diffusional mass transport.[8] As a consequence, $C_{0.0\%\ MWCNT}$ showed comparable exchange capacity to that of $C_{0.5\%MWCNT}$.

Five inorganic anions were used to test the prepared columns. Separated mixture contained iodate, bromate, nitrite, bromide, and nitrate anions. The UV detector was set at 215 nm. Comparison of the chromatography performance for separation mixture of inorganic anions on three columns using 80 mmol/L $NaClO_4$ as mobile phase were given in Figure 11.

The chromatograms (Figure 11) were obtained on three different columns with the same isocratic elution, and the operating conditions were not optimized to get reliable data for direct comparisons of the monoliths. Under these conditions, the columns containing MWCNT presented better separation efficiency for the five anions while $C_{0\%\ MWCNT}$ exhibited poor separation efficiency. It could be considered that the MWCNT provided high exchange capacity to the column as shown in Table I, thus enabling the increase in retention and resolution. Figure 3 also showed that increasing MWCNT content in the monolith to 0.5% reduced the resolution. This finding confirmed that $C_{0.5\%MWCNT}$ had lower exchange capacity than $C_{0.2\%MWCNT}$. However, $C_{0.5\%MWCNT}$ presented better resolution for the tested anions within 40 min using 70 mmol/L $NaClO_4$ as mobile phase (Figure 12). Under such condition, the lack of baseline resolution between the bromide and nitrate anions was observed in the chromatograph of $C_{0\%MWCNT}$ in Figure 12.

To compare the column efficiency in both columns, peak width at half maximum ($W_{1/2}$), plate numbers ($N$), and retention

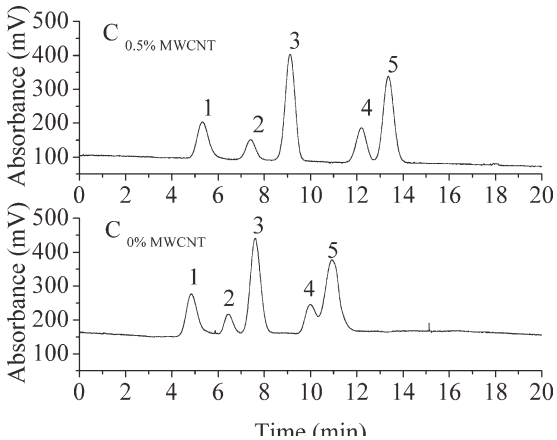


**Figure 12.** Comparison of separation of five anions on the $C_{0\%MWCNT}$ and $C_{0.5\%MWCNT}$ at 6 $\mu$L/min using 70 mmol/L $NaClO_4$ as mobile phase. Peaks identification: (1) iodate; (2) bromate; (3) nitrite; (4) bromide; (5) nitrate. Absorbance was monitored at $\lambda = 215$ nm.

**Table II.** Effect of MWCNT Content on the Column Efficiencies of $C_{0\%MWCNT}$ and $C_{0.5\%MWCNT}$ Using 70 mmol/L $NaClO_4$ as Mobile Phase at 6 μL/min

| | $C_{0\%MWCNT}$ | | | $C_{0.5\%MWCNT}$ | | |
|---|---|---|---|---|---|---|
| Anion | $W_{1/2}$ (min) | $N$ ($\times 10^4$) | $k'$ | $W_{1/2}$ (min) | $N$ ($\times 10^4$) | $k'$ |
| $IO_3^-$ | 0.48 | 0.28 | 0.60 | 0.49 | 0.32 | 2.21 |
| $BrO_3^-$ | 0.39 | 0.76 | 1.15 | 0.49 | 1.11 | 3.90 |
| $NO_2^-$ | 0.49 | 0.74 | 1.51 | 0.39 | 1.51 | 4.92 |
| $Br^-$ | - | - | 2.33 | 0.49 | 2.04 | 7.38 |
| $NO_3^-$ | 0.68 | 0.72 | 2.65 | 0.48 | 2.15 | 8.47 |

factor ($k'$) were evaluated. A summary of peak efficiencies for each of the anions was shown in Table II.

$N$ was calculated using eq. (4)[31]

$$N = \frac{5.54 \times (t_R/W_{1/2})^2}{L} \quad (4)$$

where $t_R$ was the retention time of the anion, $W_{1/2}$ was the peak width at half maximum, and $L$ was the length of the column.

$k'$ was calculated using eq. (5).[1]

$$k = \frac{t_R - t_0}{t_0} \quad (5)$$

where $t_R$ was the retention time of the anion, and $t_0$ was the dead time of the column, which was determined by the water peak.

From Table III, $W_{1/2}$ values from three anions (iodate, bromate, and nitrite anions) on $C_{0.5\%MWCNT}$ were comparable with those obtained from $C_{0\%MWCNT}$. However, the $W_{1/2}$ values from bromide and nitrate anions on $C_{0.5\%MWCNT}$ were narrower than those obtained from $C_{0\%MWCNT}$. The plate numbers ranged from 3200 to 21,500 per meter in $C_{0.5\%MWCNT}$, while those in $C_{0\%MWCNT}$ were from 2800 to 7200 per meter. Moreover, $k'$ values of both $C_{0\%MWCNT}$ and $C_{0.5\%MWCNT}$ were generally parallel to the retention order. $k'$ values from all tested anions on $C_{0.5\%MWCNT}$ were higher than those obtained from $C_{0\%MWCNT}$. These results indicated that $C_{0.5\%MWCNT}$ had superior separation efficiency, as compared with $C_{0\%MWCNT}$. Hence, comparisons of both exchange capacity and column efficiency in the two columns indicated that $C_{0.5\%MWCNT}$ provided much better ion exchange chromatographic separation of anions than $C_{0\%MWCNT}$ under the same isocratic elution condition.

The effect of $NaClO_4$ concentration in the mobile phase was also studied (Table III). If the higher concentrated mobile phase (80 mmol/L $NaClO_4$) was used, all the tested anions were analyzed within 20 min. However, these anions could not be eluted within 30 min by using the other mobile phase (30 mmol/L $NaClO_4$) in Table III. It indicated that the retention times most remarkably decreased with the $NaClO_4$ concentration in the mobile phase range from 30 mmol/L to 80 mmol/L. Furthermore, the comparison of the values in Table III showed that the highest separation efficiency in this column was obtained by using the mobile phase with a lower $NaClO_4$ concentration, though the other mobile phase was able to speed up the separations.

Finally, the relative standard deviation (RSD) for the five anions separated on $C_{0.2\%MWCNT}$ under the same condition was studied. The intraday RSD for retention time, peak area, and peak height over six runs for the five anions varied in the range of 0.3–1.6, 0.2–1.6, and 0.2–1.0%, respectively. Typically, it was anions that interacted most strongly with the stationary phase that showed the largest variation from run to run. The interday RSD for the five anions under the same conditions over 6 days were varied in the range of 1.9–2.8, 0.6–2.1, and 1.0–2.2% for retention time, peak area, and peak height, respectively. Since the injector in this study was controlled manually, it was important to maintain identical valve switching time during the separation procedure to achieve similar chromatographic properties. The columns were used daily for >2 month period without significant signs of degradation, with reproducibility studies carried out at the end of this period.

## CONCLUSIONS

The monolithic columns with and without MWCNT were synthesized via an *in situ* polymerization. The SEM micrographs indicated that MWCNT had great influence on the morphology of the monoliths. Compared with the column without MWCNT, the column containing MWCNT exhibited higher exchange capacity and better chromatographic performance. However, the experiments indicated that the $C_{0.2\%MWCNT}$

**Table III.** Effect of $NaClO_4$ Concentrations on the Column Efficiency of $C_{0.2\%MWCNT}$ at Flow Rate of 6 μL/min

| | 30 mmol/L $NaClO_4$ | | | | 80 mmol/L $NaClO_4$ | | | |
|---|---|---|---|---|---|---|---|---|
| Anion | $t_R$ (min) | $W_{1/2}$ (min) | $N$ ($\times 10^4$) | $k'$ | $t_R$ (min) | $W_{1/2}$ (min) | $N$ ($\times 10^4$) | $k'$ |
| $IO_3^-$ | 5.90 | 0.83 | 0.14 | 1.36 | 5.09 | 0.80 | 0.29 | 0.80 |
| $BrO_3^-$ | 13.88 | 0.83 | 0.77 | 4.55 | 7.80 | 0.61 | 0.53 | 1.88 |
| $NO_2^-$ | 18.29 | 0.59 | 2.66 | 6.32 | 9.91 | 1.80 | 0.96 | 2.50 |
| $Br^-$ | 27.25 | 1.31 | 1.20 | 9.90 | 13.12 | 0.70 | 1.17 | 3.84 |
| $NO_3^-$ | 32.43 | 1.07 | 2.54 | 11.97 | 15.22 | 1.61 | 1.07 | 4.67 |

showed higher exchange capacity and provided better resolution for the IC separation of five anions than $C_{0.5\%MWCNT}$. All the three monolithic columns in this study had good durability for high pressure and had good reproducibility after repeated injections. In the future, studies on the incorporation of MWCNT to polymeric monoliths, such as polystyrene and polyacrylate, will be continued.

## ACKNOWLEDGMENTS

Financial support provided by: National Natural Science Foundation of China (grant numbers: 20775070, J0830413, and 20911140271); Zhejiang Provincial Natural Science Foundation of China (grant number: R4080124); Science and Technology Project of Zhejiang Province (grant number: 2010F20012).

## REFERENCES

1. Aoki, H.; Tanaka, N.; KuBo T. *J. Polym. Sci. Part A: Polym. Chem.* **2008,** *46*, 4651.
2. Zhang, R. Y.; Yang, G. L.; Xin, P. Y. *J. Chromatogr. A* **2009,** *1216*, 2404.
3. Bedair, M.; Rassi, Z. E. *J. Chromatogr. A* **2005,** *1079*, 236.
4. Wang, H. F.; Zhu, Y. Z.; Lin, J. P. *Electrophoresis* **2008,** *29*, 952.
5. Li, Y. Y.; Tolley, H. D.; Lee, M. L. *J. Chromatogr. A* **2011,** *1218*, 1399.
6. Xin, P. Y.; Shen, Y.; Qi, L. *Talanta* **2011,** *85*, 1180.
7. Yamamoto, S.; Nakamura, M.; Tarmann, C. *J. Chromatogr. A* **2007,** *1144*, 155.
8. Chambers, S. D.; Svec, F.; Frechet, J. M. J. *J. Chromatogr. A* **2011,** *1218*, 2546.
9. Nischang, I.; Bruggemann, O. *J. Chromatogr. A* **2010,** *1217*, 5389.
10. Hutchinson, J. P.; Hilder, E. F.; Shellie, R. A. *Analyst* **2006,** *131*, 215.
11. Hutchinson, J. P.; Zakaria, P.; Bowie, A. R. *Anal. Chem.* **2005,** *77*, 407.
12. Ueki, Y.; Umemura, T.; Li, J. X. *Anal. Chem.* **2004,** *76*, 7007.
13. Nesterenkoa, E. P.; Nesterenkob, P. N.; Paull, B. *Anal. Chim. Acta* **2009,** *652*, 3.
14. Loos, M. R.; Abetz, V.; Schulte, K. *J. Polym. Sci. Part A: Polym. Chem.* **2010,** *48*, 5172.
15. Meng, F. L.; Zhang, L.; Jia, Y. *Sensor. Actuat. B: Chem.* **2011,** *153*, 103.
16. Ye, S. H.; Zhang, D.; Liu, H. Q. *J. Appl. Polym. Sci.* **2011,** *121*, 1751.
17. Khan, A. A.; Khalid, M. *J. Appl. Polym. Sci.* **2010,** *117*, 1601.
18. Niu, L. J.; Li, P.; Chen, Y. *J. Polym. Sci. Part A: Polym. Chem.* **2010,** *48*, 5172.
19. Montazer, M.; Asghari, M. S. G; Pakdel, E. *J. Appl. Polym. Sci.* **2011,** *121*, 3353.
20. Liu, H. M.; Li, J. B.; Liu, X. *Talanta* **2009,** *78*, 929.
21. Merli, D.; Speltini, A.; Ravelli, D. *J. Chromatogr. A* **2010,** *1217*, 7275.
22. Chen, J. L. *J. Chromatogr. A* **2010,** *1217*, 715.
23. Zhong, Y. Y.; Zhou, W. F.; Zhu, Y. *Talanta* **2010,** *82*, 1439.
24. Chen, J. L.; Lu, T. L.; Lin, Y. C. *Electrophores* **2010,** *31*, 3217.
25. Mayr, B.; Olzl, G. H.; Huber, K. C. G. *Anal. Chem.* **2002,** *74*, 6080.
26. Liu, Y. T.; Zhao, W.; Ye, X. Y. *Carbon* **2006,** *44*, 1613.
27. Gusev, I.; Huang, X.; Horvath, C. *J. Chromatogr. A* **1999,** *855*, 273.
28. Evenhuis, C. J.; Buchberger, W.; Pohl, C. A. *J. Sep. Sci.* **2008,** *31*, 255.
29. Ro, K. W.; Liu, J.; Knapp, D. R. *J. Chromatogr. A* **2004,** *1047*, 49.
30. Premstaller, A.; Oberacher, H.; Huber, C. G. *Anal. Chem.* **2000,** *72*, 4386.
31. Yang, J.; Yang, G. L.; Liu, H. Y. *J. Appl. Polym. Sci.* **2011,** *119*, 412.
32. Xuan, F.; Liu, J. S.; Xu, T. W. *Polym. Adv. Technol.* **2011,** *22*, 554.
33. Wu, Y. H.; Wu, C. M; Xu, T. W. *J. Appl. Polym. Sci.* **2006,** *102*, 3580.
34. Gurgel, L. V. A.; Melo, J. C. P.; Gil, L. F. *Bioresour. Technol.* **2009,** *100*, 3214.
35. Svec, F. *J. Chromatogr. A* **2010,** *1217*, 902.
36. Srinivasan, K.; Pohl, C.; Avdalovic, N. *Anal. Chem.* **1997,** *69*, 2798.
37. Gusev, I.; Huang, X.; Horvath, C. *J. Chromatogr. A* **1999,** *855*, 273.
38. Breuer, O.; Sundararaj, U. *Polym. Compos.* **2004,** *25*, 630.
39. Fernandez, R. *J. Appl. Polym. Sci.* **1984,** *29*, 341.
40. Xiao, G. L.; Fan, Y. G. *Ion Exch. Adsorp.* **2005,** *21*, 514.
41. Lu, Y. Y.; Li, H.; Liu, H. Z. *Phys. E* **2010,** *43*, 510.
42. Li, M. J.; Wang, X. B.; Tian, R. *Compos. Part A,* **2009,** *40*, 413.
43. Jiang, K.; Eitan, A.; Schadler, L. S. *Nano Lett.* **2003,** *3*, 275.
44. Kuan, H. C.; Ma, C. M.; Chang, W. P. *Compos. Sci. Technol.* **2005,** *65*, 1703.
45. Lefrant, S.; Baibarac, M.; Baltog, I. *J. Mater. Chem.* **2009,** *19*, 5690.